Vegetable Research

ARTICLE

Open Access

https://doi.org/10.48130/vegres-0026-0032

Vegetable Research **2026**, 6: e039

Misregulation of strigolactones receptor *DWARF14* leads to altered plant architecture in tomato

Yan Han[1,2#], Fengze Sun[2#], Ge Wang[2,3], Xiaofei Qin[2], Fangfang Ma[2*] and Zhilong Bao[2*]

[1] *Taishan Vocational and Technical College, Tai'an, Shandong 271000, China*
[2] *College of Horticulture Science and Engineering, Shandong Agricultural University, Tai'an, Shandong 271018, China*
[3] *College of Agriculture and Biology, Liaocheng University, Liaocheng, Shandong 252059, China*
[#] Authors contributed equally: Yan Han, Fengze Sun
[*] Correspondence: fma@sdau.edu.cn (Ma F); zbao@sdau.edu.cn (Bao Z)

Abstract

The strigolactone (SL) receptor *DWARF14* (*D14*) is a key negative regulator of shoot branching; however, its contribution to architectural variation in tomato remains unclear. In this study, a comprehensive analysis integrating axillary bud phenotypes, *SlD14* expression levels, and promoter *cis*-regulatory element structures was conducted using 10 determinate and 10 indeterminate tomato cultivars. The results revealed a close association between *SlD14* expression and variation in axillary bud development, suggesting a potential role for *SlD14* in regulating tomato branching architecture. Tissue-specific expression analysis revealed that *SlD14* was predominantly expressed in the shoot apex and stem tissues, while subcellular localization assays showed that *SlD14* was mainly localized in the nucleus and cytoplasm. To further validate its biological function, CRISPR/Cas9-mediated *sld14* knockout mutants were generated in tomato. Loss of *SlD14* function significantly promoted the emergence and elongation of axillary shoots, resulting in a highly branched phenotype characterized by reduced plant height, enlarged leaf angle, and altered plant architecture. Transcriptome analysis further revealed that altered *SlD14* expression caused extensive transcriptional reprogramming of multiple phytohormone signaling pathways, particularly auxin-responsive genes (*SAUR*, *AUX*, and *ARF*), gibberellin metabolism-related genes (*GA2ox*), and brassinosteroid signaling components (*BES1/BZR1*). Collectively, these findings demonstrate that precise regulation of *SlD14* is essential for maintaining axillary bud dormancy and apical dominance, and that its misregulation disrupts hormonal homeostasis, leading to enhanced axillary shoot outgrowth. This study provides new molecular insights into tomato architectural variation and identifies *SlD14* as a promising target for breeding improved plant architecture.

Keywords: *DWARF14*; Tomato; Strigolactones; Plant architecture; Lateral branches; Leaf angle

Citation: Han Y, Sun F, Wang G, Qin X, Ma F, et al. 2026. Misregulation of strigolactones receptor *DWARF14* leads to altered plant architecture in tomato. *Vegetable Research* 6: e039 https://doi.org/10.48130/vegres-0026-0032

Introduction

Plant architecture is a key agronomic trait that strongly influences crop productivity, cultivation management, and ornamental value[1]. It is determined by multiple characteristics, including plant height, branching pattern, inflorescence architecture, and leaf angle. Among these traits, lateral branching plays a central role in shaping overall plant architecture by affecting light interception, spatial distribution, and reproductive development. For gramineous crops, effective tillering (the formation of lateral branches at the base of the stem) determines the number of panicles and directly affects the yield, while reducing ineffective tillering is conducive to the rational use of nutrients[2–4]. While branching is a key yield determinant in cereal crops, its role in ornamental species is primarily focused on canopy compactness and aesthetic value. For ornamentals, branching has an important impact on visual effects[5]. Branching is an important feature of plant architecture, as well as the result of axillary bud initiation and bud growth, and has a decisive effect on the seed yield of cash crops[6,7]. As an important plant architecture index, the leaf angle directly affects the distribution of light and CO_2 in the canopy and the light energy utilization of the population, which further affects the process of plant growth and development, physiological characteristics, and finally affects the yield[8–11]. Branch development of plants is a very important link in the growth process, and the number and angle of branches are important factors in determining crop plant architecture, and are also related to crop development, yield, and cultivation mode[12]. The branching characteristics of plants are influenced by many factors, including plant nutrition, growth and development stage, endogenous hormones, environment, epigenetic factors, and transcription factors[13,14].

Among the various endogenous signals, strigolactones (SLs) have emerged as a class of novel phytohormones that primarily inhibit axillary bud outgrowth. Strigolactones were initially isolated from the root exudates of cotton (*Gossypium hirsutum*)[15,16]. To date, numerous natural strigolactones (SLs) have been identified in plants. Based on their structural characteristics, natural SLs are generally classified into canonical and non-canonical strigolactones. Canonical SLs mainly include strigol- and orobanchol-type compounds, whereas non-canonical SLs possess structural variations in the core SL scaffold[17–19]. SLs are a novel plant hormone that inhibits the growth and development of lateral buds and regulates plant branching[20,21]. The *D14-MAX2-D53* signaling module serves as the core mechanism for SL perception and signal transduction. Rice *D14* homologous genes, such as Arabidopsis *D14*, petunia *DAD2*, and pea *RMS3*, encode a hydrolase that hydrolyzes SLs[22,23]. D14 is an atypical hormone receptor that plays a key role in the SL signaling pathway. It is a substrate specifically recognized by leucine-rich repeat F-box protein MAX2/D3, which leads to ubiquitination and degradation of the substrate[24,25]. The *D14* gene has been functionally analyzed in many plants[26,27]. The *d53* and *d14* mutants have similar phenotypes of dwarfing and multiple tillers, and through the

© The Author(s)

https://doi.org/10.48130/vegres-0026-0032

analysis of multiple branching mutants in Arabidopsis, rice, pea, and other model plants, remarkable progress has been made in the molecular mechanism of SLs' regulation of plant branching.

The SL pathway suppressor SMAX1-LIKE in *Arabidopsis thaliana* and the F-box protein MAX2 (the homologous protein in rice is D3) are involved in SL-mediated plant branching regulation. SLs can enhance the interaction of D14 with MAX2 and D53, while MAX2 can remove the inhibition of D53 on the SL signaling pathway through ubiquitination and degradation of D53, thus activating the expression of downstream genes and regulating normal plant branching[28,29]. The *sld14* mutant obtained by CRISPR/Cas9 technology showed decreased plant height and root biomass, increased branching, and changed leaf shape compared with wild-type plants. At the same time, the mutant leaves were light green, chlorophyll and carotenoid contents were decreased, chloroplast structure was abnormal, and photosynthesis was weakened. The results indicated that the SL receptor gene *SlD14* not only modulates the development of roots, stems, branches, and leaves, but also plays a role in regulating photosynthetic pigment accumulation and photosynthetic capacity[30].

To investigate the molecular basis underlying axillary shoot emergence in tomato, we comparatively analyzed plant architecture traits between 10 determinate and 10 indeterminate tomato cultivars and identified lateral branching as a major factor contributing to architectural variation. Integrated analyses of branching phenotypes, *SlD14* expression patterns, and promoter *cis*-regulatory element composition revealed that differential expression of *SlD14*, a key receptor in SL signaling, was closely associated with axillary bud outgrowth, suggesting that misregulation of *SlD14* contributes to the emergence of axillary shoots in tomato. To further validate its biological function, CRISPR/Cas9-mediated gene editing was employed to generate two homozygous *sld14* mutants in the indeterminate tomato cultivar 34#. Phenotypic characterization demonstrated that disruption of *SlD14* significantly promoted axillary shoot emergence and elongation, leading to excessive branching accompanied by reduced plant height and altered leaf angle. Furthermore, transcriptome sequencing analysis revealed that altered *SlD14* expression triggered extensive transcriptional reprogramming in multiple phytohormone signaling pathways, particularly auxin, gibberellin, and brassinosteroid-related genes. Collectively, these findings demonstrate that misregulation of *SlD14* disrupts hormonal homeostasis and promotes axillary shoot emergence, thereby reshaping tomato plant architecture.

Materials and methods

Plant materials and growth conditions

In this study, 20 experimental tomato materials with determinate and indeterminate growth characteristics were generated by our research group. The following 10 determinate tomato varieties were used: 'Barbara Tomato' (BL), 'Dwarf Red Bell' (AR), 'Tomato Pink Bird' (F), 'Balconi Yellow' (BK), 'Canary' (J), 'Yellow Cherry Tomato' (HY), 'Tomato Redbird' (R), 'Dwarf Red Bell' (AH), 'Red Pearl Tomato' (RZ), and 'Micro Tom' (MT). Ten indeterminate tomato varieties; laboratory codes 104#, 30#, 34#, 353#, 36#, 114#, 334#, 49#, 331#, and 17#, were used with 10 biological replicates each. Transgenic experiments were carried out with background materials of the tomato variety laboratory code 34#. The seeds were disinfected in 75% alcohol for 1 min, disinfected in 8% sodium hypochlorite solution for 15 min, washed with high-temperature sterilized water five times, and planted on MS medium supplemented with 0.7% AGAR. The cotyledons were fully developed, transplanted into a matrix of vermiculite mixed with nutrient soil (2:1), and cultured in the plant culture room. The day and night temperatures of the growth chamber were 25/22 °C, the light duration was 16 h, the dark duration was 8 h, and the light intensity was 275 μmol·m^{-2}·s^{-1}. Once the plants grew to the five-leaf stage, the fifth compound leaf was frozen in liquid nitrogen and stored for real-time fluorescence quantitative PCR (RT–qPCR) analysis to determine the tissue expression specificity of *SlD14* at the transcript level.

Subcellular localization

The full-length coding sequence (CDS) of *SlD14* without the stop codon was amplified and cloned into the pGWB405 vector to generate the SlD14-GFP fusion construct. The GFP vector was used as the empty-vector control. The recombinant plasmids were introduced into *Agrobacterium tumefaciens* strain GV3101 and transiently expressed in *Nicotiana benthamiana* leaves by agroinfiltration. The bacterial suspension was infiltrated into the leaves of 4–6-week-old *N. benthamiana* plants using a needleless syringe. After infiltration, the plants were maintained under normal growth conditions for 48–72 h. GFP fluorescence was observed using a confocal laser scanning microscope (Zeiss LSM880) to determine the subcellular localization of SlD14. At least three independent biological replicates were performed for each construct.

Construction of the *SlD14* CRISPR vector and genetic transformation of tomato

The knockout vector was constructed using the CRISPR/Cas9 gene editing system. pG3K-U6SC was used in this study. After cloning and assembling the CRISPR expression cassette, the resulting products were transformed into *Escherichia coli* (heat shock method), verified by primers U6-29p-F and U6-29p-R; positive colonies were screened and sequenced, and the extracted plasmids were subsequently transformed into *A. tumefaciens* LA4404 harboring the helper plasmids pVS1-VIR2 (electric shock method)[31]. The primers used in the present study were synthesized by Tsingke Biological Co., Ltd. (Qingdao, China).

The tomato cultivar 34#, as described above, was used as the wild-type background for genetic transformation. The wild-type seeds were sown and disinfected on a sterile table, and the seeds with full particles were evenly sown on MS medium, with 25 seeds per bottle. After dark treatment for 3 d, the seeds were germinated and were placed in the culture room with unchanged parameters. When the cotyledons fully developed, the middle part of the cotyledon was cut as the explant, and the explants were placed on the medium with the axial side down for 2 d in the dark at 28 °C. Afterwards, the activated *Agrobacterium* solution was prepared, *Agrobacterium* infection was carried out on a superclean table, and then co-culture, differentiation culture, and rooting culture were carried out. For verification of the tomato transgenic lines, the CTAB method was used for DNA extraction; expression cassette primers were used to verify whether the expression cassette was transferred, and the gene fragment primers *SlD14*-T1-F and *SlD14*-T2-R were used to verify whether gene editing was successful. If there was no significant difference, sequencing was performed for verification.

RNA extraction and RT-qPCR analysis

Total RNA was extracted by the TRIzol method; the RNA concentration was measured by a spectrophotometer, and the integrity of

the RNA was detected by agarose gel electrophoresis. cDNA was extracted using the HiScript II 1st Strand cDNA Synthesis Kit (+g DNA wiper) DNA kit. The reverse transcription products were detected by PCR, and RT–qPCR analysis was performed using a ChamQTM Universal SYBR® qPCR Master Mix (Vazyme) Kit (Nanjing Vazyme Biological Co., Ltd.). The operation was carried out according to the instructions of the $2^{-\Delta\Delta CT}$ method for data analysis[32].

Measurement of physiological parameters

The physiological indices of 80-d-old determinate tomato, indeterminate-growth tomato, and 60-d-old WT and transgenic lines were determined. The number of lateral branches and nodes was counted, and the length of lateral branches and nodes, leaf length, and leaf width were measured with a straight ruler. Plant height, stem diameter, plant width, leaf angle, opening angle, drooping angle, and leaf area were measured using ImageJ software after the fixed camera took photos, using the default parameters.

SlD14 promoter cloning and sequencing

Genomic DNA was extracted from 20 tomato cultivars using the cetyltrimethylammonium bromide (CTAB) method. The *SlD14* promoter regions were amplified from genomic DNA and cloned into the pAbAi vector. Recombinant plasmids were sequenced using Sanger sequencing with multiple sequencing primers, and the resulting sequence reads were assembled to obtain the complete *SlD14* promoter sequences for each cultivar.

Protein extraction and western blot analysis

Total proteins were extracted from young leaves of wild-type (WT) and sld14 mutant plants using a protein extraction buffer supplemented with a protease inhibitor cocktail. Equal amounts of total protein were separated by SDS-PAGE and transferred onto a PVDF membrane. The membrane was blocked with 5% skim milk in TBST for 1 h at room temperature and then incubated overnight at 4 °C with a SlD14-specific primary antibody (PhytoAB, Cat. PHY8025A). After washing three times with TBST, the membrane was incubated with a secondary antibody for 1 h at room temperature. Following three washes with TBST, the protein signals were detected using an enhanced chemiluminescence (ECL) detection system.

Transcriptome analysis

RNA was extracted from the stem tips of wild-type and *SlD14* knockout mutant tomato lines *sld14* cr-1 and *sld14* cr-2 at 40 d of age, and transcriptome analysis was performed. There were three groups with three biological replicates per group, and a total of nine samples were sequenced by RNA-Seq. Transcriptome sequencing and analysis were performed by Lingen Biotechnology, Inc. (www.biozeron.com). Gene annotations and channels were downloaded (https://mapman.gabipd.org/home).

Data analysis

The mapping software and data processing software used in this study included Microsoft Excel and the R language. The statistical software DPS7.05[33] and Duncan's test were used to analyze the significance of differences in the obtained data, and different letters indicate significant differences ($p < 0.05$).

Results

Natural variation in tomato plant architecture across cultivars

Twenty tomato cultivars, including 10 determinate and 10 indeterminate types, exhibited extensive natural variation in plant architecture. At the whole-plant level, these germplasms displayed highly diverse phenotypic patterns, particularly in lateral shoot development and leaf morphology (Fig. 1a–c; Supplementary Figs. S1 and S2). Quantitative analyses further confirmed these observations, revealing significant differences ($p < 0.05$) among the 20 cultivars in key architectural traits, including lateral branch length, number of lateral branches, internode length, and node number (Fig. 1d–g; Supplementary Fig. S3). It is noteworthy that certain cultivars (e.g., 'BL') exhibited strong branching capacity, whereas others (e.g., '17' and '30') showed almost complete suppression of lateral branch formation. In addition, pronounced variation in internode elongation was also observed across cultivars. Collectively, the wide-ranging differences in branching patterns and stem development indicate substantial genetic diversity underlying tomato plant architecture in these materials.

Differences in leaf architecture between determinate and indeterminate tomato growth types

Leaf angles at the 3rd, 5th, and 7th nodes in the lower, middle, and upper canopy were measured after plants reached a stable growth stage. As shown in Supplementary Fig. S4, determinate-type tomato cultivars exhibited consistently larger leaf angles than indeterminate growth types across all canopy positions. Similar trends were observed for leaf opening angle and leaf drooping angle (Supplementary Fig. S4). Across canopy positions, drooping angle showed a gradual decrease from lower to upper nodes, but this positional pattern was consistent in both growth types. Overall, determinate tomato cultivars displayed a flatter leaf architecture compared with indeterminate growth tomatoes.

Phenotypic and transcriptional characterization of *SlD14* reveals its association with tomato plant architecture variation

To elucidate the role of *SlD14* in regulating tomato plant architecture, we integrated phenotypic evaluation, transcriptional profiling, promoter *cis*-regulatory analysis, and trait correlation across 20 tomato accessions (Fig. 2). Significant natural variation in *SlD14* transcript abundance was detected by RT-qPCR, with accession '49' exhibiting the highest expression and 'J' and '34' showing the lowest levels (Fig. 2a). This variation in expression was closely associated with differences in axillary shoot development, particularly branch initiation timing, which ranged from approximately 30 to over 70 d among accessions (Fig. 2b), indicating a potential relationship between *SlD14* activity and the regulation of bud outgrowth dynamics. Correlation analysis further revealed that *SlD14* expression was significantly and negatively correlated with the number of lateral branches (NOB), as well as upper leaf opening angle (UOA) and upper leaf drooping angle (UDA) (Fig. 2c), whereas no significant correlations were observed with general growth-related traits such as stem diameter (SD), leaf width (LW), or leaf area (LA). These results suggest that *SlD14* is more specifically involved in the regulation of branching architecture and leaf spatial configuration rather than overall vegetative biomass accumulation. To investigate the potential regulatory basis of this expression divergence, promoter

https://doi.org/10.48130/vegres-0026-0032

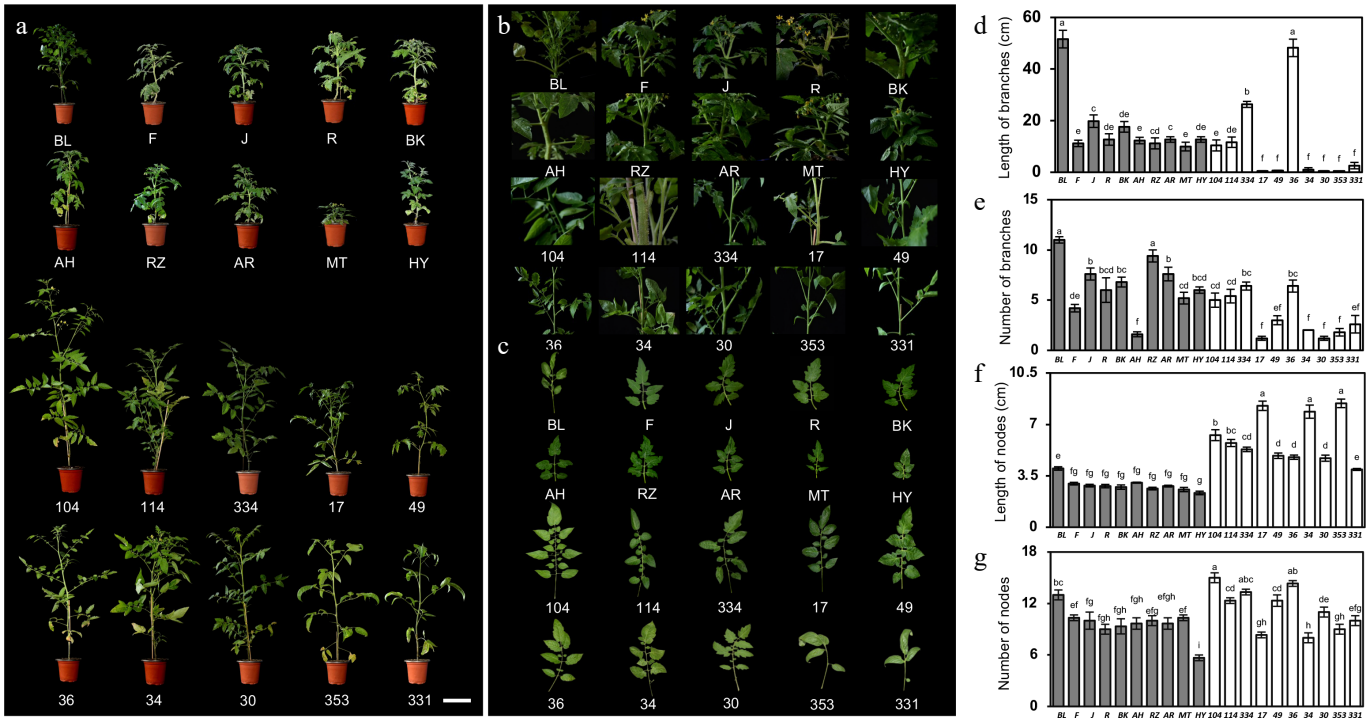


Fig. 1 Variation in lateral branch and internode traits among 20 tomato cultivars. (a) Overall morphology of 20 tomato varieties: Scale bar = 10 cm. (b) Lateral branch development phenoarchitecture of 20 tomato species. (c) Leaf development phenoarchitecture of 20 tomato species. Quantitative analysis of branch and internode traits: (d) branch length, (e) number of branches, (f) internode length, and (g) number of internodes. Data are presented as mean ± SE. Different lowercase letters above the bars indicate significant differences among accessions according to Duncan's multiple range test ($p < 0.05$).

analysis of the approximately 2 kb upstream region of *SlD14* across all accessions revealed a largely conserved *cis*-regulatory architecture enriched in light-, ABA-, MeJA-, auxin-responsive, and meristem-associated elements (Fig. 2d), indicating that sequence variations leading to the loss of several *cis*-regulatory motifs were detected in some accessions, suggesting expression divergence may result from subtle promoter variation rather than extensive structural differences (Fig. 2d). Collectively, these findings demonstrate that natural variation in *SlD14* expression is closely associated with differences in axillary branching and leaf angle traits, supporting its role in shaping tomato plant architecture.

Subcellular localization and tissue-specific expression analysis of *SlD14*

We analyzed the tissue-specific expression of *SlD14* in tomato using RT-qPCR. The gene was expressed in all examined tissues, including root, stem, leaf, and shoot apex, with the highest expression levels detected in the shoot apex and leaves, while relatively lower expression was observed in the roots (Fig. 3a). To investigate the subcellular localization of the SlD14 protein, we generated a SlD14-GFP fusion construct and transiently expressed it in the abaxial epidermal cells of *N. benthamiana* leaves. As shown in Fig. 3b, the fluorescence signal of the SlD14-GFP fusion protein was observed in both the cytoplasm and the nucleus, indicating dual subcellular localization. In contrast, free GFP used as a control was distributed uniformly throughout the cell (Fig. 3b).

CRISPR/Cas9-mediated mutagenesis and functional characterization of *SlD14* in tomato

To obtain material with loss of function in tomato *SlD14* mutants, we designed two targets for the *SlD14* gene via CRISPR/Cas9 gene-editing technology (Fig. 4a). The tomato cultivar 34#, as described above, was used as the wild-type background for genetic transformation. We produced more than 10 heterozygous mutants from the T0 generation through *LBA4404-Agrobacterium*-mediated tomato genetic transformation. After screening in the T1 generation, two mutant lines were selected in the T2 generation. The lines were named *sld14* cr-1 and *sld14* cr-2, respectively. The sequencing results showed that *sld14* cr-1 had a 2 bp deletion in Target 1 and a 3 bp deletion and a 2 bp substitution in Target 2, resulting in a frameshift mutation. This leads to early termination of protein transcription. There is a 1 bp insertion in Target1 of the *sld14* cr-2 line and a 1 bp substitution and a 1 bp deletion in Target 2 (Fig. 4a), which also leads to a frameshift mutation and early termination of protein transcription, resulting in loss of function of the *SlD14* protein. In addition, a SlD14-specific antibody was used to detect SlD14 protein accumulation, and the SlD14 protein signal was markedly reduced or undetectable in the mutant lines compared with the WT, further confirming the loss-of-function of *SlD14* (Fig. 4c). We examined the selected transgenic lines for the presence of Cas9 by genomic PCR and assessed potential off-target mutations (Supplementary Fig. S5). These analyses confirmed that the transgenic plants used in this study were free of the Cas9 transgene/protein and showed no detectable edits at the predicted off-target loci. Meanwhile, we detected the gene expression of *SlD14* in the WT and mutant lines, and the results showed that the expression of *SlD14* in the mutant lines was lower than that in the WT (Fig. 4b).

SlD14 knockout alters tomato plant architecture

At 60 d after transplantation, the *sld14* knockout mutants (cr-1 and cr-2) exhibited obvious architectural alterations compared

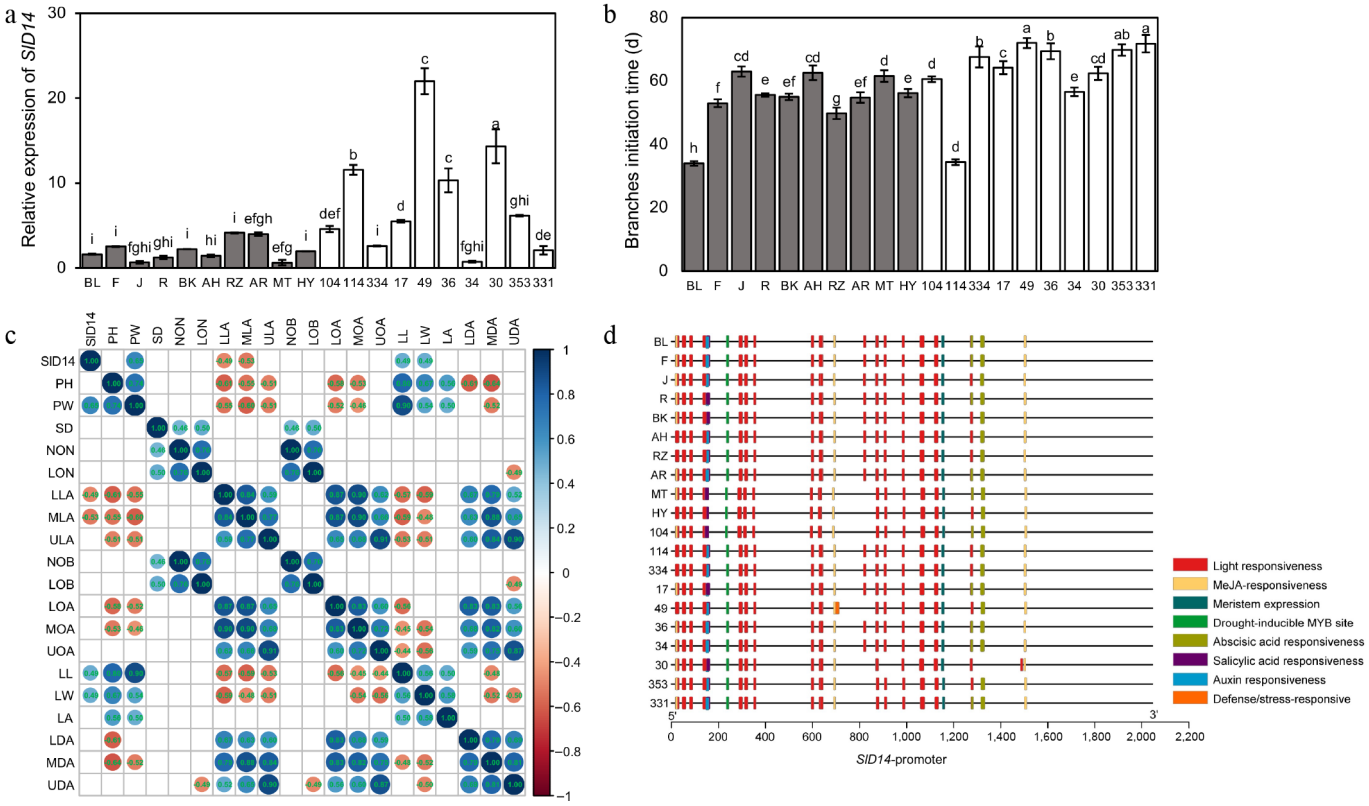


Fig. 2 Expression and promoter analysis of *SlD14* and integrated analysis of *SlD14* expression and plant growth traits. (a) Relative expression of *SlD14* in all 20 tomato varieties. Data are presented as mean ± SE. Different lowercase letters above the bars indicate significant differences among accessions according to Duncan's multiple range test ($p < 0.05$). (b) Variation in branch initiation time (d) among 20 tomato cultivars. (c) Correlation analysis between *SlD14* expression and plant architecture-related traits in 20 tomato plants. The following data were collected: plant height (PH), plant width (PW), number of nodes (NON), length of nodes (LON), stem diameter (SD), number of lateral branches (NOB), length of lateral branches (LOB), upper, middle, and lower leaf angles (ULA, MLA, LLA), upper, middle, and lower opening angle (UOA, MOA, LOA), upper, middle, and lower drooping angles (UDA, MDA, LDA), leaf length (LL), leaf width (LW), and leaf area (LA). (d) Analysis of *cis*-regulatory elements in the SlD14 promoters of the 20 cultivars Supplementary Table S1.

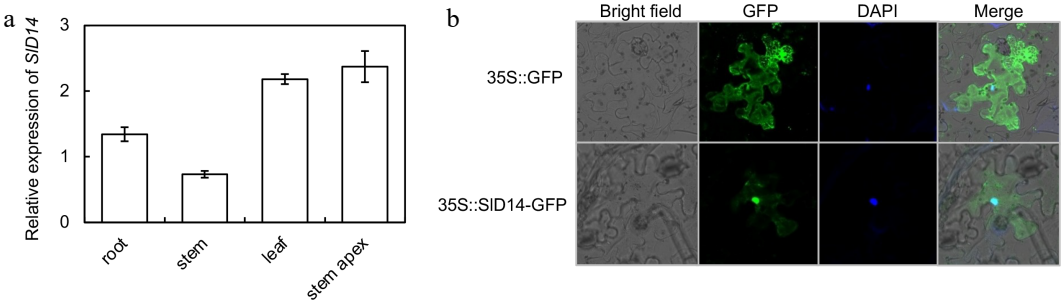


Fig. 3 Expression patterns and subcellular localization of *SlD14* in tomato. (a) *SlD14* expression in different tomato tissues. Data are presented as mean ± SE. (b) Subcellular localization of 35S::SlD14-GFP in abaxial epidermal cells of tobacco leaves, with 35S::GFP alone as a control.

with wild-type (WT) plants, including reduced plant size and enhanced branching (Fig. 5a, f, k). Quantitative analysis showed that plant height was significantly decreased in the *sld14* mutants relative to WT plants (Fig. 5b), while no significant difference in node number was detected among the genotypes (Fig. 5c). In contrast, internode length was markedly reduced in the mutant lines (Fig. 5d), indicating that the dwarf phenotype mainly resulted from shortened internodes rather than reduced node formation. Plant width was also significantly lower in *sld14* plants than in WT plants (Fig. 5e). Moreover, stem diameter was significantly increased in the mutant lines (Fig. 5h), suggesting enhanced stem thickening following *SlD14* disruption. Branching-related traits were strongly affected by *SlD14* knockout, as both the number and length of lateral branches were significantly higher in the mutants than in WT plants (Fig. 5j, l). In addition, the mutants displayed significantly reduced leaf length and leaf area compared with WT plants (Fig. 5m, o), whereas leaf width showed no significant difference among the genotypes (Fig. 5n). Together, these results demonstrate that *SlD14* plays an essential role in regulating tomato plant architecture, particularly in controlling plant height, internode elongation, and lateral branching.

https://doi.org/10.48130/vegres-0026-0032

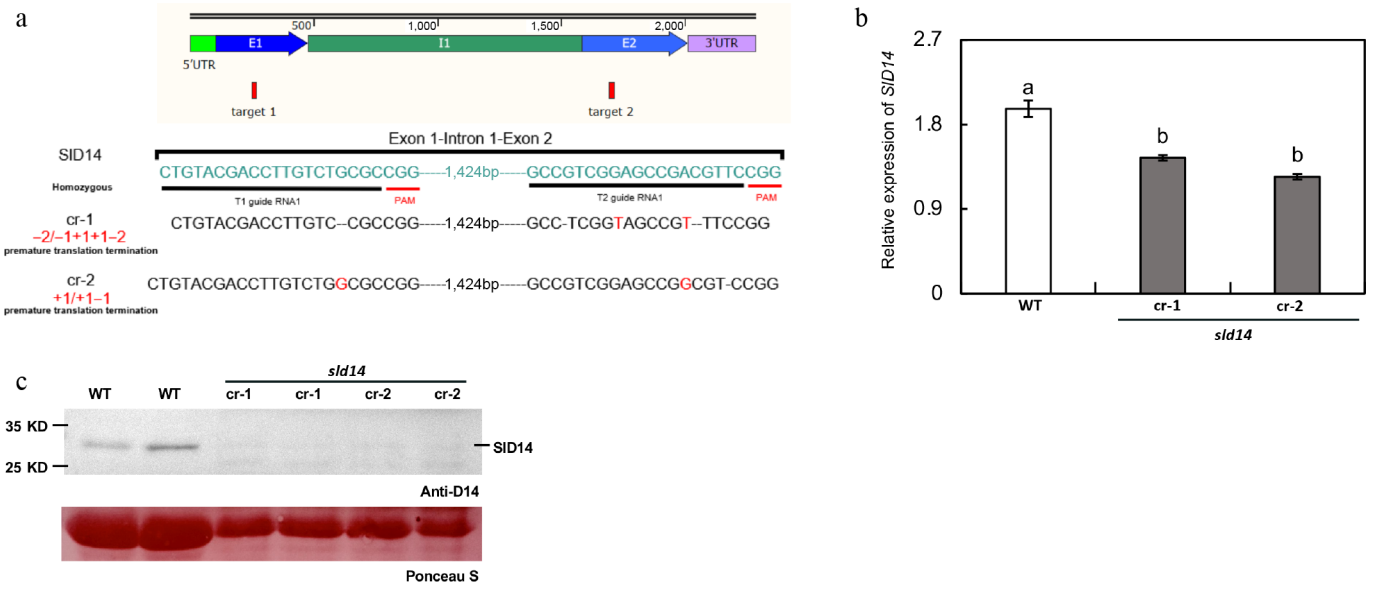


Fig. 4 Sequence and expression analysis of *SlD14* in CRISPR/Cas9 knockout tomato lines. (a) Alignment of *SlD14* sequences from wild-type (WT) and transgenic knockout lines, highlighting insertions, deletions, and other mutations. Differences from the WT sequence are indicated in red. (b) Relative expression levels of *SlD14* in WT and knockout lines. (c) Western blot analysis of SlD14 protein levels in WT, sld14 cr-1, and sld14 cr-2 plants using a SlD14-specific antibody. Data are presented as mean ± SE. Different lowercase letters above the bars indicate significant differences among accessions according to Duncan's multiple range test ($p < 0.05$).

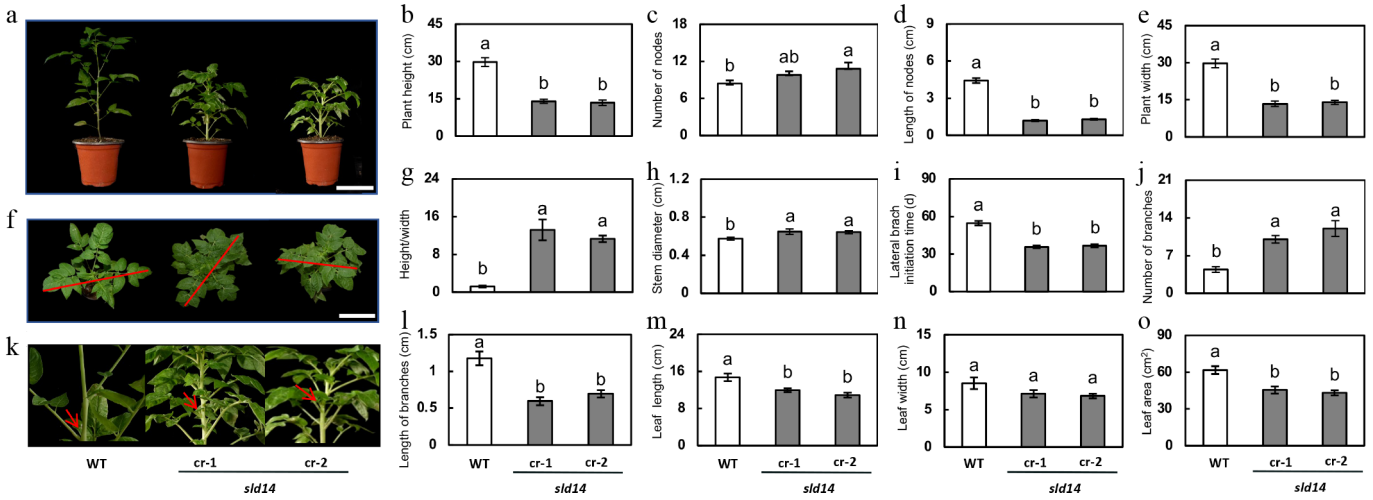


Fig. 5 Morphology of 60-day-old *SlD14* knockout and WT tomato seedlings. Morphology of 60-day-old *SlD14* knockout (*sld14*) and wild-type (WT) tomato seedlings, shown in (a) front view, (f) top view, and (k) branching pattern, illustrating clear differences in overall architecture; scale bar = 10 cm. Red arrows indicate the positions of lateral buds or branches. (b) Plant height, (c) number of nodes, (d) length of nodes, (e) plant width, (g) plant height/width ratio, (h) stem diameter, (i) lateral branch initiation time, (j) number of lateral branches, (l) length of lateral branches, (m) leaf length, (n) leaf width, and (o) leaf area of WT and *SlD14* mutant lines (*sld14* cr-1 and cr-2). Data are presented as mean ± SE. Different lowercase letters above the bars indicate significant differences among accessions according to Duncan's multiple range test ($p < 0.05$).

SlD14 regulates the development of plant leaf angles in tomato

The two SlD14 mutant lines exhibited significant changes in leaf architecture compared with WT plants. Leaf angle measurements at the 3rd, 5th, and 7th nodes showed that mutants consistently displayed larger leaf angles across all canopy positions, with increases of 13.3%, 9.5%, and 30.9% in the lower, middle, and upper leaves, respectively, relative to WT. Consistent with this trend, leaf opening angle showed a position-dependent response: no significant difference was detected in the lower leaves, whereas significant increases were observed in the middle and upper leaves, by 25% and 45%, respectively (Supplementary Fig. S6). A similar pattern was also found for leaf drooping angle, which showed only a minor, non-significant increase of 6.5% in the lower leaves but significant increases of 36% and 45% in the middle and upper canopy, respectively. Overall, SlD14 disruption primarily affected leaf angle traits in the middle and upper canopy, resulting in a more horizontally expanded leaf architecture compared with WT plants.

RNA-seq analysis of *SlD14* mutants and WT plants

To investigate the molecular mechanisms underlying the altered architecture of *sld14* mutants, comparative transcriptome

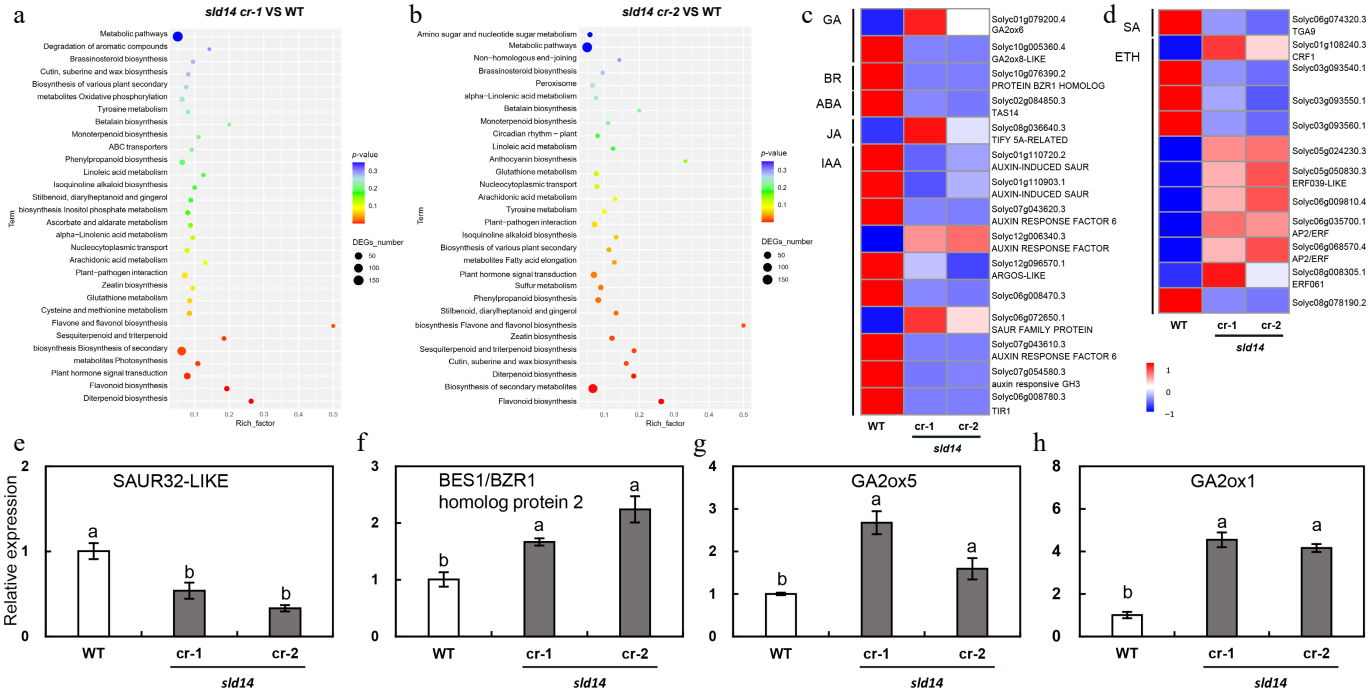


Fig. 6 RNA-seq analysis of the *SlD14* mutants and WT plants. (a), (b) KEGG analysis revealed that the biosynthesis of secondary metabolites, plant hormone signaling pathways, metabolic pathways, plant–pathogen interaction pathways, karyotoplasmic transport, and phenylpropanoid biosynthesis were significantly enriched in both groups. (c), (d) The expression analysis of DEGs related to the synthesis of auxin, jasmonic acid, gibberellin, abscisic acid, brassinosteroid, salicylic acid, and ethylene. (e)–(h) Relative expression levels of SAUR32-like, BES1/BZR1 homolog protein 2, GA2ox5, and GA2ox1 in WT, sld14 cr-1, and sld14 cr-2 plants, as determined by RT-qPCR. Data are presented as mean ± SD. Different lowercase letters above the bars indicate significant differences among accessions according to Duncan's multiple range test ($p < 0.05$).

analyses were performed between the two independent knockout lines and WT plants (Fig. 6; Supplementary Fig. S7). KEGG enrichment analysis revealed that the differentially expressed genes (DEGs) in both *sld14 cr-1* and *sld14 cr-2* were significantly enriched in multiple pathways, including biosynthesis of secondary metabolites, metabolic pathways, flavonoid biosynthesis, diterpenoid biosynthesis, phenylpropanoid biosynthesis, and plant hormone signal transduction (Fig. 6a, b). In addition, pathways related to plant–pathogen interaction, nucleocytoplasmic transport, and lipid metabolism were also significantly enriched in the mutant lines (Fig. 6a, b), indicating that disruption of *SlD14* broadly affected cellular metabolism and signaling processes. Hormone-related expression profiling further demonstrated that numerous genes associated with gibberellin (GA), brassinosteroid (BR), abscisic acid (ABA), jasmonic acid (JA), and auxin (IAA) biosynthesis or signaling were differentially expressed in the *sld14* mutants compared with WT plants (Fig. 6c). Moreover, genes involved in salicylic acid (SA) and ethylene (ETH) pathways also displayed obvious transcriptional changes in the mutants (Fig. 6d). To further validate the transcriptome results, the expression patterns of four representative hormone-related genes, SAUR32-like, BES1/BZR1 homolog protein 2, gibberellin 2-oxidase 5 (GA2ox5), and gibberellin 2-oxidase 1 (GA2ox1), were examined by RT-qPCR. The RT-qPCR results were consistent with the transcriptome data, supporting the reliability of the RNA-seq analysis (Fig. 6e–h). Collectively, these results suggest that *SlD14* regulates tomato plant architecture through extensive modulation of hormone signaling pathways and secondary metabolic processes.

Discussion

Plant architecture is a complex quantitative trait determined by the coordinated regulation of stem elongation, branching dynamics, and leaf spatial configuration. In this study, substantial variation in *SlD14* transcript abundance exists among diverse tomato germplasms. Interestingly, promoter analysis revealed that the upstream regulatory region of *SlD14* is highly conserved and enriched with multiple hormone-responsive and light-responsive *cis*-elements, suggesting that expression divergence is likely driven by subtle regulatory modulation rather than major promoter structural variation. This observation implies that upstream transcription factors, epigenetic modifications, or environmental signaling pathways may contribute to the differential expression of *SlD14* among tomato accessions. Notably, most determinate cultivars exhibited relatively lower *SlD14* expression than indeterminate cultivars, implying a potential association between reduced *SlD14* activity and the establishment of compact growth habits in tomato. Because branching architecture and leaf angle are critical determinants of cultivation suitability, planting density adaptation, and ornamental value, natural variation in *SlD14* expression may represent an important genetic resource for tomato breeding. Moderate manipulation of *SlD14* activity could therefore provide a strategy to optimize canopy structure, improve planting density adaptation, and enhance determinate traits in tomato.

SlD14 encodes the strigolactone (SL) receptor, which functions as a core component of SL signaling to suppress axillary bud outgrowth and regulate shoot architecture. Consistent with this role, strong negative correlations between *SlD14* expression and lateral branch number, as well as upper leaf opening and drooping angles,

https://doi.org/10.48130/vegres-0026-0032

indicate that variation in *SlD14* transcript abundance is closely linked to natural architectural differentiation. Modulation of SLs' perception capacity, rather than complete pathway disruption, may underlie the phenotypic diversification between determinate and indeterminate growth types. Collectively, these observations indicate that fine-tuning *SlD14* transcript levels is an important mechanism for reshaping tomato canopy architecture. Reduced *SlD14* expression in determinate cultivars may weaken SLs-mediated suppression of axillary bud outgrowth, thereby contributing to the compact and highly branched growth pattern characteristic of determinate tomatoes.

Functional analysis further demonstrated that *SlD14* regulates multiple developmental processes beyond branch suppression. In addition to enhanced branching, *sld14* mutants exhibited significant reductions in plant height, internode length, plant width, and leaf angle, indicating that *SlD14* coordinately regulates overall plant morphology. Importantly, node number was not significantly altered in the mutants, suggesting that the dwarf phenotype primarily resulted from inhibition of internode elongation rather than reduced node initiation. Similar phenotypic effects have been reported in SL-deficient or SL-insensitive mutants in rice, Arabidopsis, and pea, where impaired SL signaling leads to compact plant architecture and excessive tillering or branching[34]. The increased stem diameter observed in the mutants may reflect altered carbon allocation or compensatory radial growth caused by reduced vertical elongation. Moreover, the reduction in leaf angle observed in *sld14* plants suggests that *SlD14* also participates in regulating leaf spatial configuration, which may ultimately influence light interception efficiency and canopy structure. Together, these results demonstrate that *SlD14* coordinately controls shoot branching, stem elongation, and leaf architecture to shape tomato plant architecture.

To further elucidate the molecular basis underlying these phenotypic changes, transcriptome analysis revealed that *SlD14* functions as an important regulatory hub integrating multiple hormone signaling pathways. Transcriptomic analysis revealed that *SlD14* participates in multiple hormonal pathways and mediates complex hormonal crosstalk to fine-tune tomato architecture. SL signaling has been proposed to restrict bud activation by modulating auxin canalization and sink strength[35,36]. SLs and IAA interact in regulating plant branching[37]. Our observation of the hyper-branching phenotype in *sld14* mutants reinforces this model within the context of tomato development. The pronounced branching phenotype in *sld14* mutants supports the hypothesis that intact *SlD14*-mediated signaling is required to maintain apical dominance in tomato. In addition, internode length decreased markedly in the mutants, suggesting that *SlD14* influences not only meristematic activity but also cell elongation processes. Therefore, the reduced plant height in *sld14* mutants is unlikely to be solely a secondary consequence of altered branching competition but likely reflects direct or indirect regulation of elongation growth. Additionally, the increased stem diameter in mutants may indicate compensatory changes in vascular development or altered carbon allocation under enhanced branching pressure.

Transcriptomic analysis also suggested that gibberellin (GA) and brassinosteroid (BR) pathways may participate in *SlD14*-mediated architectural regulation. GA negatively regulates the expression of transcription factors OSH1 and TB1 in rice, and these two genes regulate the occurrence of meristem and the growth of lateral buds, respectively, so GA can suppress tillering[38,39]. The significant upregulation of *SlGA2ox*, a key gene involved in GA catabolism, suggests that mutation of *SlD14* may reduce bioactive GA accumulation, which may contribute to the altered branching pattern[40,41]. Brassinosteroids (BRs) are essential plant hormones that regulate diverse aspects of plant growth and development, including cell elongation, reproductive development, and senescence[42,43]. In this study, we found that the *SlD14* mutation can cause downregulation of BES1/BZR1 expression. This suggests that *SlD14* may influence tomato branching architecture through modulation of BR signal transduction. The decrease in the expression of BRI1-EMS-suppressor (BES1), the positive regulator of BR signaling, and its homologous gene can significantly inhibit the multi-branch phenotype of max2 mutants[6].

To our knowledge, this study provides one of the first systematic analyses linking natural variation in SlD14 expression with architectural divergence between determinate and indeterminate tomato germplasms. Optimizing plant architecture is a major objective in modern tomato breeding because compact growth habits, appropriate branching patterns, and suitable leaf angle are closely associated with high-density cultivation, mechanized cultivation, and ornamental quality. The phenotypic characteristics of *sld14* mutants observed in this study, including enhanced lateral branching and reduced plant stature, suggest that *SlD14* represents a valuable candidate gene for molecular breeding. Precise regulation of *SlD14* expression in commercial tomato cultivars may facilitate optimizing branch architecture and canopy openness, thereby improving canopy light distribution and potentially contributing to yield stability. Future studies focusing on natural allele mining, promoter engineering, and the interaction networks of *SlD14* will further facilitate its application in tomato architectural improvement and breeding programs.

Conclusions

In summary, we systematically characterized the role of *SlD14* in regulating tomato plant architecture. By analyzing 20 tomato accessions, we found that natural variation in *SlD14* expression is closely associated with differences in branching traits and leaf spatial configuration, particularly in lateral branch number, branch initiation timing, and leaf angle- related traits. Through CRISPR/Cas9-mediated knockout of *SlD14*, we further demonstrated that loss of its function leads to a compact plant architecture characterized by reduced plant height and internode length, increased lateral branching, and altered leaf morphology, including decreased leaf angle. In addition, transcriptome analysis revealed that these phenotypic changes are accompanied by extensive transcriptional reprogramming, especially in plant hormone signaling pathways and secondary metabolism. Taken together, these results indicate that *SlD14* plays a central role in coordinating axillary branching and canopy architecture by integrating hormonal and developmental signals, thereby shaping overall tomato plant growth form.

Author contributions

The authors confirm their contributions to the paper as follows: conceptualization, methodology: Han Y, Sun F, Bao Z, Ma F; writing – original draft: Han Y, Sun F, Bao Z, Ma F; editing – original draft: Sun F, Bao Z, Ma F; validation: Han Y, Sun F, Bao Z, Ma F, Wang G; investigation: Han Y, Sun F, Bao Z, Ma F, Wang G, Qin X. All authors reviewed the results and approved the final version of the manuscript.

Data availability

The original contributions presented in the study are included in the article; further inquiries can be directed to the corresponding authors.

Acknowledgments

We gratefully acknowledge the support of the National Natural Science Foundation of China (32573059). We thank the College of Horticulture Science and Engineering at Shandong Agricultural University for supporting the Experimental Core Facilities, where we performed phenotypic analysis and plant culture.

Conflict of interest

The authors declare that they have no conflict of interest.

Supplementary information accompanies this paper online at: https://doi.org/10.48130/vegres-0026-0032.

Dates

Received 1 June 2026; Revised 26 August 2026; Accepted 17 September 2026; Published online 17 November 2026

References

[1] Teichmann T, Muhr M. 2015. Shaping plant architecture. *Frontiers in Plant Science* 6:233

[2] Wang Y, Li J. 2011. Branching in rice. *Current Opinion in Plant Biology* 14:94–99

[3] Guo W, Chen L, Herrera-Estrella L, Cao D, Tran LSP. 2020. Altering plant architecture to improve performance and resistance. *Trends in Plant Science* 25:1154–1170

[4] Takai T. 2024. Potential of rice tillering for sustainable food production. *Journal of Experimental Botany* 75:708–720

[5] Garbez M, Galopin G, Sigogne M, Favre P, Demotes-Mainard S, et al. 2015. Assessing the visual aspect of rotating virtual rose bushes by a labeled sorting task. *Food Quality and Preference* 40:287–295

[6] Hu J, Sun S, Wang X. 2020. Regulation of shoot branching by strigolactones and brassinosteroids: conserved and specific functions of *Arabidopsis* BES1 and rice BZR1. *Molecular Plant* 13:808–810

[7] Gu J, Struik PC, Evers JB, Lertngim N, Lin R, et al. 2024. Quantifying differences in plant architectural development between hybrid potato (*Solanum tuberosum*) plants grown from two types of propagules. *Annals of Botany* 133:365–378

[8] Pierik R, Fankhauser C, Strader LC, Sinha N. 2021. Architecture and plasticity: optimizing plant performance in dynamic environments. *Plant Physiology* 187:1029–1032

[9] Guo J, Li W, Shang L, Wang Y, Yan P, et al. 2021. *OsbHLH98* regulates leaf angle in rice through transcriptional repression of *OsBUL1*. *New Phytologist* 230:1953–1966

[10] Cao Y, Dou D, Zhang D, Zheng Y, Ren Z, et al. 2022. ZmDWF1 regulates leaf angle in maize. *Plant Science* 325:111459

[11] Yang X, Li R, Jablonski A, Stovall A, Kim J, et al. 2023. Leaf angle as a leaf and canopy trait: Rejuvenating its role in ecology with new technology. *Ecology Letters* 26:1005–1020

[12] Ward SP, Leyser O. 2004. Shoot branching. *Current Opinion in Plant Biology* 7:73–78

[13] Evers JB, van der Krol AR, Vos J, Struik PC. 2011. Understanding shoot branching by modelling form and function. *Trends in Plant Science* 16:464–467

[14] Chen Z, Chen Y, Shi L, Wang L, Li W. 2023. Interaction of phytohormones and external environmental factors in the regulation of the bud dormancy in woody plants. *International Journal of Molecular Sciences* 24:17200

[15] Cook CE, Whichard LP, Turner B, Wall ME, Egley GH. 1966. Germination of witchweed (*Striga lutea* Lour.): isolation and properties of a potent stimulant. *Science* 154:1189–1190

[16] Wang L, Smith SM. 2016. Strigolactones redefine plant hormones. *Science China Life Sciences* 59:1083–1085

[17] Guercio AM, Palayam M, Shabek N. 2023. Strigolactones: diversity, perception, and hydrolysis. *Phytochemistry Reviews* 22:339–359

[18] Mashiguchi K, Seto Y, Yamaguchi S. 2021. Strigolactone biosynthesis, transport and perception. *The Plant Journal* 105:335–350

[19] Jia KP, Baz L, Al-Babili S. 2018. From carotenoids to strigolactones. *Journal of Experimental Botany* 69:2189–2204

[20] Al-Babili S, Bouwmeester HJ. 2015. Strigolactones, a novel carotenoid-derived plant hormone. *Annual Review of Plant Biology* 66:161–186

[21] Fiorilli V, Forgia M, de Saint Germain A, D'Arrigo G, Cornu D, et al. 2022. A structural homologue of the plant receptor D14 mediates responses to strigolactones in the fungal phytopathogen *Cryphonectria parasitica*. *New Phytologist* 234:1003–1017

[22] de Saint Germain A, Clavé G, Badet-Denisot MA, Pillot JP, Cornu D, et al. 2016. An histidine covalent receptor and butenolide complex mediates strigolactone perception. *Nature Chemical Biology* 12:787–794

[23] Yao R, Ming Z, Yan L, Li S, Wang F, et al. 2016. DWARF14 is a non-canonical hormone receptor for strigolactone. *Nature* 536:469–473

[24] Tal L, Palayam M, Ron M, Young A, Britt A, et al. 2022. A conformational switch in the SCF-D3/MAX2 ubiquitin ligase facilitates strigolactone signalling. *Nature Plants* 8:561–573

[25] Gu P, Tao W, Tao J, Sun H, Hu R, et al. 2023. The D14-SDEL1-SPX4 cascade integrates the strigolactone and phosphate signalling networks in rice. *New Phytologist* 239:673–686

[26] Liu T, Zhang X, Zhang H, Cheng Z, Liu J, et al. 2022. *Dwarf and High Tillering1* represses rice tillering through mediating the splicing of *D14* pre-mRNA. *The Plant Cell* 34:3301–3318

[27] Zhang C, Wang F, Jiao P, Liu J, Zhang H, et al. 2024. The overexpression of *Zea mays* strigolactone receptor gene *D14* enhances drought resistance in *Arabidopsis thaliana* L. *International Journal of Molecular Sciences* 25:1327

[28] Liang Y, Ward S, Li P, Bennett T, Leyser O. 2016. SMAX1-LIKE7 signals from the nucleus to regulate shoot development in Arabidopsis via partially EAR motif-independent mechanisms. *The Plant Cell* 28:1581–1601

[29] Kodama K, Xie X, Kyozuka J. 2023. The D14 and KAI2 orthologs of gymnosperms sense strigolactones and KL mimics, respectively, and the signals are transduced to control downstream genes. *Plant & Cell Physiology* 64:1057–1065

[30] Li Z, Pi Y, Zhai C, Xu D, Ma W, et al. 2022. The strigolactone receptor SlDWARF14 plays a role in photosynthetic pigment accumulation and photosynthesis in tomato. *Plant Cell Reports* 41:2089–2105

[31] Zhang Q, Zhang Y, Lu MH, Chai YP, Jiang YY, et al. 2019. A novel ternary vector system united with morphogenic genes enhances CRISPR/Cas delivery in maize. *Plant Physiology* 181:1441–1448

[32] Livak KJ, Schmittgen TD. 2001. Analysis of relative gene expression data using real-time quantitative PCR and the $2^{-\Delta\Delta CT}$ method. *Methods* 25:402–408

[33] Tang QY, Zhang CX. 2013. Data Processing System (DPS) software with experimental design, statistical analysis and data mining developed for use in entomological research. *Insect Science* 20:254–260

[34] Pandey A, Sharma M, Pandey GK. 2016. Emerging roles of strigolactones in plant responses to stress and development. *Frontiers in Plant Science* 7:434

[35] Zhang J, Mazur E, Balla J, Gallei M, Kalousek P, et al. 2020. Strigolactones inhibit auxin feedback on PIN-dependent auxin transport canalization. *Nature Communications* 11:3508
[36] Rameau C, Bertheloot J, Leduc N, Andrieu B, Foucher F, et al. 2015. Multiple pathways regulate shoot branching. *Frontiers in Plant Science* 5:741
[37] Wang Q, Smith SM, Huang J. 2022. Origins of strigolactone and karrikin signaling in plants. *Trends in Plant Science* 27:450–459
[38] Lo SF, Yang SY, Chen KT, Hsing YI, Zeevaart JA, et al. 2008. A novel class of gibberellin 2-oxidases control semidwarfism, tillering, and root development in rice. *The Plant Cell* 20:2603–2618
[39] Takai T, Taniguchi Y, Takahashi M, Nagasaki H, Yamamoto E, et al. 2023. *MORE PANICLES 3*, a natural allele of *OsTB1/FC1*, impacts rice yield in paddy fields at elevated CO_2 levels. *The Plant Journal* 114:729–742
[40] Ritonga FN, Zhou D, Zhang Y, Song R, Li C, et al. 2023. The roles of gibberellins in regulating leaf development. *Plants* 12:1243
[41] Katyayini NU, Rinne PLH, Tarkowská D, Strnad M, van der Schoot C. 2020. Dual role of gibberellin in perennial shoot branching: inhibition and activation. *Frontiers in Plant Science* 11:736
[42] Clouse SD, Sasse JM. 1998. BRASSINOSTEROIDS: essential regulators of plant growth and development. *Annual Review of Plant Physiology and Plant Molecular Biology* 49:427–451
[43] Nolan TM, Vukašinović N, Liu D, Russinova E, Yin Y. 2020. Brassinosteroids: multidimensional regulators of plant growth, development, and stress responses. *The Plant Cell* 32:295–318

Copyright: © 2026 by the author(s). Published by Maximum Academic Press, Fayetteville, GA. This article is an open access article distributed under Creative Commons Attribution License (CC BY 4.0), visit https://creativecommons.org/licenses/by/4.0/.